AN ASSESSMENT OF VOID FRACTION DATA WITH COBRA-IE

D.L. Aumiller and M.J. Meholic
Bettis Atomic Power Laboratory
PO Box 79
West Mifflin, PA 15122 USA
david.aumiller@unnpp.gov

ABSTRACT

COBRA-IE is a three-field sub-channel analysis code under development at the Bettis Atomic Power Laboratory. The analysis code is being developed as a general purpose thermal-hydraulic analysis tool with an emphasis on use in an integrated code system for analyzing postulated Large Break Loss-of-Coolant-Accidents.

The overall accuracy of programs such as COBRA-IE is tied to the ability to predict void fraction. As such, a comprehensive assessment has been made using one-dimensional void fraction data. The results of this assessment are provided in this report. The assessment utilizes data from 9 different experimental facilities. It includes data from air-water and steam-water facilities, heated flow, adiabatic flow, subcooled boiling, saturated boiling, co-current up flow and co-current down flow. Approximately 1100 data points are evaluated and included in this assessment. Overall, COBRA-IE was able to predict the void fraction with an average error (predicted – experimental) of less than 0.04. Plots describing the relationship between the error in the prediction and parameters such as pressure and flow are also provided.

KEYWORDS
Void Fraction Assessment, subcooled boiling

1. INTRODUCTION

Interfacial drag and its impact on void fraction is an important part of any two-fluid analysis code for steady-state, transient and reactor safety applications [1-3]. Unfortunately, there are no direct measurement techniques for interfacial drag. Instead, the adequacy and accuracy of these important models are assessed through the comparison of predicted void fraction data to experimental data. This approach is appropriate given that the volumetric make up of a two-phase mixture is intrinsically important to many phenomena of interest in the thermal-hydraulic of reactors under both steady-state and transient conditions. For instance, for commercial pressurized water reactors (PWRs), the presence of boiling can influence both total and local power. Additionally, during the reflood phase of a light-water reactor, the void fraction that exists below the quench front will directly impact the location of the quench front and hence the coolability of the fuel rod.

There are a wide range of conditions for which interfacial conditions can be important in the thermal-hydraulic analyses of light water reactors. While most of the conditions of interest exhibit co-current up-flow of the two-phase mixture, during the blowdown phase of a Loss-of-Coolant Accident (LOCA), co-current down-flow is important to the cooling of the reactor. Additionally, while boiling conditions in the reactor are clearly important, there are conditions which are either nearly adiabatic such as the inlet plenum during a LOCA or for which the heat transfer to the fluid is limited to the conduction time scale for thick metal structures such as the downcomer fluid volumes. Assessment of experimental data that

covers all of these conditions is required to demonstrate the adequacy of the analysis tools and methods for application to reactor analyses.

2. COBRA-IE Model Set

While a complete description of the physical model sets is outside of the scope of the current paper, a very brief description of the important models in the calculation of the void fraction is provided here. COBRA-IE is a variant of the COBRA-TF analysis code [4]. As such, it uses a three-field approach where the evolution of the entrained droplet field is calculated through the application of mechanistic entrainment and depositions models which are based on the local flow characteristics. The interfacial topology of the liquid-vapor interface is determined by the application of a static flow regime map that is a function of the void fraction.

In order to provide continuous closure relationships, COBRA-IE uses a process where the interfacial terms are calculated for three different flow regimes (pure small bubble, pure large bubble and annular), and the results are then interpolated to provide the conditions of interest. The flow regime definitions are included in Table I. To show how the elemental models are combined in COBRA-IE, the various contributions of the small bubble, large bubble and annular flow models are plotted as a function of void fraction in Figure 1. The following sections will provide a description of the flow regimes and the calculation of the interfacial shear in each.

Table I – Flow Regime Identification and Logic

Flow Regime	Description	Range
Single Phase Liquid	---	$\alpha_g < 0.0001$
Transition	---	$0.0001 < \alpha_g < 0.001$
Small Bubble	Dispersed bubbly	$0.001 < \alpha_g < 0.2$
Small-to-Large Bubble Transition	Presence of both small and large bubbles. Volume fraction weighting of the contribution of each bubble type. No entrained droplets.	$0.2 < \alpha_g < 0.5$
Churn-Turbulent	Transition region between bubbly and annular. Volume fraction weighting of the contribution of each regime.	$0.5 < \alpha_g < 0.8$
Unstable Annular	Liquid film with disturbance waves. Entrainment of liquid droplets from the film can occur by various mechanisms.	$0.8 < \alpha_g < 0.999$
Stable Annular	Thin liquid film without disturbance waves. No Entrainment from films.	$0.8 < \alpha_g < 0.999$
Transition	---	$0.999 < \alpha_g < 0.9999$
Single Phase Vapor	---	$0.9999 < \alpha_g$

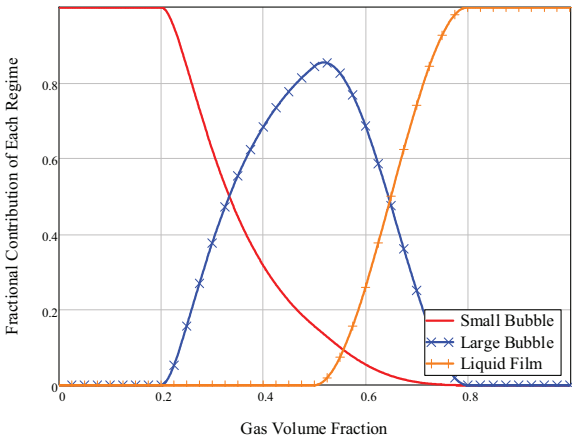

Figure 1 – Contributions of Different Physical Model Sets as a Function of Void Fractions.

2.1 Small Bubble Regime

The calculation of interfacial shear for the small bubble regime uses either the Clift-Gauvin model [5] or the original COBRA-TF models for distorted bubbles and cap bubbles as described in Reference [4]. In this regime, the interfacial area is calculated using a critical Weber number of 10 and with a relative velocity that is calculated as the minimum of the phasic relative velocity as calculated by COBRA-IE and the maximum plausible bubble rise velocity.

2.2 Large Bubble Regime

For large bubbles, the Clift-Gauvin model [5] is modified to account for bubble swarm effects.

$$C_{D,LB} = \left[C_{D,CG}(\mathrm{Re}_{LB})\right](1-\alpha)^2 \tag{1}$$

In this regime, the interfacial area is calculated using the model of Kitscha [6]. The equivalent diameter for the bubbles is calculated using:

$$D_{LB} = 0.6788\left\{27.07L_{cap}\left[1+N_{\mu}\right]^{0.83}\right\} \tag{2}$$

where the Laplace capillary length, L_{cap}, is equal to:

$$L_{cap} = \sqrt{\frac{\sigma}{g\left(\rho_{l,avg}-\rho_{g,avg}\right)}} \tag{3}$$

and the viscosity number, N_{μ}, is equal to

$$N_{\mu} = \frac{\mu_{l,avg}}{\sqrt{\rho_{l,avg}\sigma L_{cap}}} \tag{4}$$

2.3 Annular Regimes

One of the regions where COBRA-IE has been fundamentally improved relative to COBRA-TF has been in the accuracy, consistency and robustness of the annular flow models. The new models have been described in detail in References [7-8]. The models use a two-zone method whereby the interfacial shear on the film is calculated by superimposing the interfacial drag associated with waves onto the interfacial shear for a smooth base film. The fraction of time that waves are present on a surface, called intermittency, is calculated from an empirical relationship. There are two different entrainment mechanisms that have been developed in this model set. Each of the models uses the interfacial shear from the two-zone model as input. The first model is associated with roll-wave stripping and the second is for Kelvin-Helmholtz lifting. References [7-8] provide a comparison of the new models with 254 steam-water and 55 air-water experimental data points. A statistical analysis shows that the improved modeling package reduces the mean relative error in the predicted axial pressure gradient from 108% to 6% (both overprediction) for the high-pressure steam–water cases considered. Predictions of the outlet entrained fraction indicate the new modeling package reduces the mean relative error from 20% (underprediction) to 4.5% (overprediction) for the 254 high and low pressure steam–water cases considered.

2.4 Large Open Regions

The impact of walls on interfacial shear and void fractions has been well established [9-10]. In an effort to improve interfacial shear predictions for large regions, a combination of the Kataoka-Ishii [11] and the Zuber-Findley [12] drift-flux correlations has been implemented in COBRA-IE. This method was chosen in part because the RELAP5-3D code [13] utilizes a similar approach for vertically oriented pipes with hydraulic diameters in excess of 8 cm. The RELAP5-3D formulation of the correlations has been adopted. The drift flux formulation is converted to an equivalent interfacial drag coefficient which is used for the small bubble and large bubble flow regimes for sub-channels that have been identified as large open regions. The smoothing between the pure small bubble, pure large bubble and annular regimes are the same for these sub-channels as described above.

2.5 Boiling Heat Transfer

Some of the experiments that are used in this assessment involve subcooled and saturated boiling. The boiling curve methodology of COBRA-TF has been retained in COBRA-IE. The Chen correlation [14] is used to calculate the heat transfer coefficients for both subcooled and saturated nucleate boiling. The code has been modified such that the boiling incipience model of Steiner-Taborek as described in Reference [15] is used to transition between the single-phase convection and boiling. The addition of this model was required as the previous model could use non-physical boiling heat transfer coefficients in conditions where there was heat transfer from the liquid to the wall as a result of greater superheat being present in the liquid than present at the surface of the fuel rod.

3 Experimental Data used in Assessment

A database of open literature, steady-state, void fraction data has been cataloged for the purpose of assessing the interfacial drag models in COBRA-IE. Data sets that include more prototypic rod bundle geometry introduce the effects of single-phase and two-phase mixing. Since this assessment is intended to focus on interfacial shear, it will focus on approximately 1100 data points from 9 different experimental facilities that represent flow in a tube or a duct. The resulting data set includes cases with both co-current up-flow and co-current down-flow, cases with both steam-water and air-water working fluids, and both

adiabatic and boiling conditions. For the boiling conditions, data for both subcooled and saturated nucleate conditions is included in the assessment.

The range of conditions for the various data sets has been included in Table II. For each test, the working fluid, number of data points used, and the ranges for pressure, the absolute value of the mass flux, the superficial velocities and the hydraulic diameter are given. For the heated facilities, the ranges of superficial velocities represent the calculated superficial velocities at each point where experimental data was provided. Two facility data sets, Bhagwat and Petrick, have co-current down-flow. These have been highlighted in the superficial velocity entries in the table.

The range of conditions examined is quite extensive. The hydraulic diameter range extends from 6.3 mm to 175 mm. The Smith and Takeuchi data are large enough to use the drift flux formulation. All of the other facilities utilize the default models in COBRA-IE. Examining just the heated tests, the pressure range extends from 1 -15 MPa and the mass fluxes extend from 406 - 2125 $\frac{kg}{m^2 s}$.

Table II - Range of Conditions for Experiments Used in Assessment

	Data Set	Fluid	Number of Points	Pressure (MPa)	Abs Mass Flux $\left(\frac{kg}{m^2 s}\right)$	Void Fraction (-)	j_l $\left(\frac{m}{s}\right)$	j_g $\left(\frac{m}{s}\right)$	D (mm)
Adiabatic	Smith	Air-Water	93	0.10-0.13	50-2005	0.026-0.714	0.049-2.000	0.042-10.19	102-152
	Bhagwat		193	0.11 – 0.24	56-2374	0.025-0.912	-2.381 - -0.053	-20.27 - -0.052	12.7
	Beattie	Steam-Water	36	7	639-2598	0.242-0.864	0.286-3.415	0.755-24.02	73.9
	Petrick		89	4.1-6.9	193-1121	0.092-0.808	-1.37 - -0.229	-1.517- -0.022	49.3
	Takeuchi		6	6.9	366-531	0.400-0.840	0.390-0.570	0.609-5.368	175
Heated	Christensen	Steam-Water	112	2.8 - 6.9	640-940	0.005-0.650	0.739-1.170	0.000-2.069	17.8
	Bartolomey		272	3.0 - 15.0	406-2125	0.000-0.584	0.486-3.325	0.000-2.677	12.0
	Sabotinov		40	6.8	417-960	0.013-0.795	0.398-1.225	0.007-4.984	11.7
	Marchaterre		266	1.0 - 4.2	494-1527	0.003-0.756	0.538-1.828	0.000-7.294	11.3

The following sections will provide a brief description of each of the test facilities.

3.1 Smith

This was an adiabatic, co-current up-flow, air-water facility [16]. All of the data is taken at atmospheric pressure. Two different size tubes were investigated in this data set. The void fraction range covers the bubbly and churn-turbulent flow regimes in COBRA-IE. The data is taken using conductivity probes.

The local data is then integrated to determine the area averaged data that is used in this assessment. For each run, data is collected at three different elevations.

3.2 Bhagwat

This was an adiabatic, co-current down-flow, air-water facility [17]. All of the data is taken at atmospheric pressure. The void fraction range covers all of the flow regimes in COBRA-IE. The void fraction is measured with a set of quick acting valves that captures a two-phase mixture within the test section. The amount of liquid trapped between the valves was measure which permitted the void fraction to be determined. For each of the 193 runs, a single data point is collected. In the following figures, this data is designated as OSU, for the location where the thesis was published (Oklahoma State University).

3.3 Beattie

This was an adiabatic, co-current up-flow, steam-water facility [18]. All of the data is taken at a pressure of 7 MPa. A total of 36 simulations are included in the assessment with a single data point provided for each run. Most of the data represents annular or near annular conditions. The void fraction was measured using a gamma densitometer.

3.4 Petrick

This was an adiabatic, co-current down-flow, steam-water facility [19]. A total of 89 simulations are provided for this facility; a single comparison is made for each simulation. The pressure range for this facility extended from 4 - 7 MPa. The void fraction that is presented was taken using pressure differential data that was validated using 2 independent techniques.

3.5 Takeuchi

This was an adiabatic, co-current up-flow, steam-water facility [20]. This facility was designed to examine conditions consistent with two-phase flow in the riser section of a PWR. This facility has the largest diameter of any of the facilities examined. There are only 6 data points, all taken at 6 MPa, provided in the reference; each is treated as an independent simulation in the current assessment. The void fractions examined are mostly in the churn-turbulent regime in COBRA-IE.

3.6 Christensen

This test facility was a boiling, co-current up-flow facility [21]. This test utilized a rectangular duct that had a 44.4 x 11.1 mm flow area. The pressure range for the experiments extended from 2.8 - 6.9 MPa. The void fraction was measured at 16 different axial locations in the test section using gamma densitometry. A total of 7 simulations were performed yielding 112 data points.

3.7 Marchaterre

This heated boiling test facility utilized two different rectangular test sections [22] and included data for both forced and natural convection. Only the data from the 6.3 x 51 mm test section in forced flow is examined in the current assessment. The test series used gamma densitometry to measure the void fraction at 10 axial locations within the test section.

3.8 Bartolomey and Sabotinov

The data from these boiling experiments was taken from Reference [23]. The data is taken in heated tubes. The void fraction is obtained with gamma densitometry. The authors of Reference [23] state that the experimental uncertainty for the cases is 4%. A wide range of pressures (3 - 15 MPa) and mass fluxes are included in these data sets. The diameters for each facility are similar (12.0 v. 11.7 mm). The void fractions examined covered all but the annular flow regimes.

4. Execution of Cases

The use of automated systems for verification, validation and assessment of reactor safety codes is the most effective method for performing these tasks. The process that has been described in Aumiller [24] for the automated verification of COBRA-IE has also been used in assessment processes described in this paper. The `make` utility has been chosen as the driver for the automated process. This choice was predicated on the following:

- It can perform parallel operations and requires no setup of this feature.
- Its use of targets and dependencies can be exploited to identify sub-sets of the problems that can be built up to form the entirety of the required testing.
- It is widely available on computing platforms.
- It provides an extensible platform such that new cases are easily added.

The execution for each data point starts with a base input deck that can vary by experimental facility. The base input deck contains information concerning the nodalization, boundary condition locations and timestep information. The process then obtains information about the specific boundary conditions and initial conditions for the run from a file containing all of the information for the test series. This data is then substituted into the base deck, and the simulation is performed. COBRA-IE can only be executed as a transient analysis code; as such, the boundary conditions are established and simulations are allowed to reach the conditions where the time averaged conditions are not varying. The simulation results are then time averaged over the final portion of the transient to obtain the data provided on the plots. The process to perform the 415 simulations requires less than 5 minutes when executed using the parallel capabilities of `make` on a single node with 16 processors.

Some of the subcooled experimental data was provided as plots of void fraction as a function of equilibrium quality. Since the COBRA-IE void fraction is calculated as a function of position, a method is needed to calculate the void fraction at the specified experimental qualities. To do this, the mass flow weighted experimental quality was calculated for each of the volumes within the COBRA domain. Using this data, the predicted void fraction data was interpolated to the experimental quality values. This interpolated void fraction is then compared to the experimentally determined values.

All of the cases used cell lengths of approximately 10 cm. Nodalization studies were performed for each of the test series; the comparisons to void fraction data were shown to be insensitive to additional reductions in cell length.

5. Results

The comparison of the error in the void fraction data is shown as a histogram in Figure 2. The data shows that mean error in void fraction prediction ($\alpha_{pred} - \alpha_{exp}$) over the wide range of conditions is 0.038. This represents a slight bias toward over predicting the void fraction data. The standard deviation in the error is 0.094. A single plot containing all of the data predictions is presented in Figure 3. The figure shows the data is congregated around the line indicating perfect prediction. The bias toward overestimating the void fraction is evident in the figure.

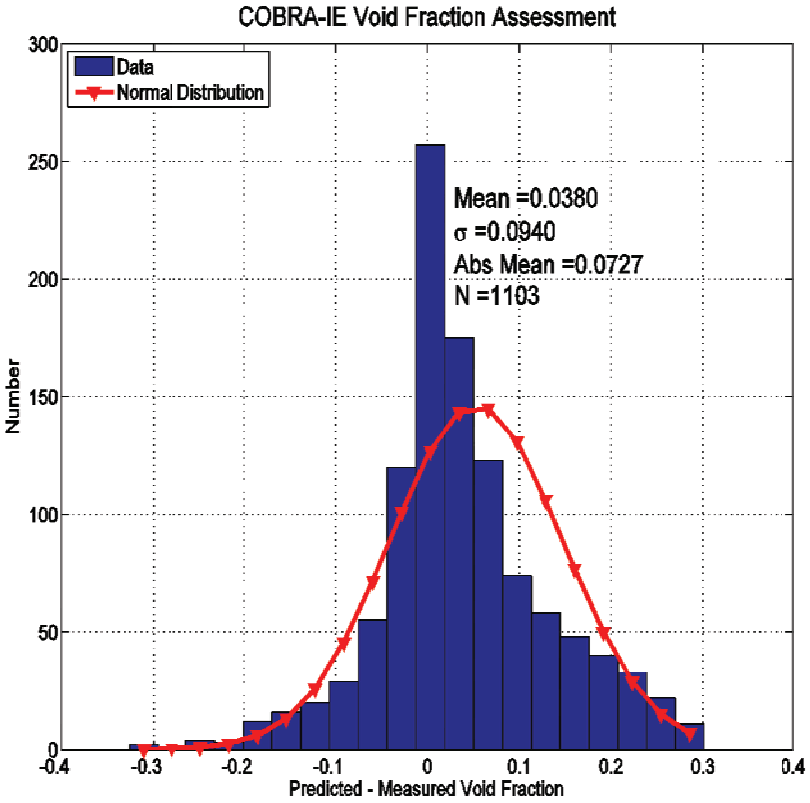

Figure 2 – Histogram of Error in Void Fraction Predictions

A table highlighting the results from all of the data is presented in Table III. There are several interesting points that can be seen from the comparisons. The first is that, on average, the errors for adiabatic tests, mean error of -0.02, are closer to zero than for the heated tests, mean error of 0.074. The standard deviation for the error for both data sets is the same. When examined at this level, the data seems to indicate a potential bias in the calculations of the void fraction for heated cases. When the heated data is examined more closely, it is apparent that the Marchaterre data is significantly influencing the statistics for this subset. The range of conditions for the Marchaterre data, taken in a duct, is within the range of conditions for the Christensen (duct) and Bartolomey (tube) tests; both of which are predicted more accurately. This eliminates the geometry of the test section as the cause of the differences in the accuracy of the COBRA-IE predictions.

Table III – Compilation of Results from Void Assessment

	Data Set	Fluid	Number of Points	Mean Error	RMS Error	Mean Abs Val Error	Std Dev of Error
Adiabatic	Smith	Air-Water	93	-0.072	0.12	0.093	0.097
	Bhagwat		193	-0.017	0.051	0.033	0.049
	Beattie	Steam-Water	36	-0.088	0.107	0.094	0.062
	Petrick		89	0.058	0.091	0.077	0.071
	Takeuchi		6	-0.079	0.097	0.093	0.061
All Adiabatic			417	-0.02	0.086	0.062	0.083
Heated	Christensen	Steam-Water	112	0.022	0.045	0.034	0.04
	Bartolomey		269	0.022	0.044	0.032	0.038
	Sabotinov		40	0.039	0.067	0.048	0.054
	Marchaterre		272	0.127	0.15	0.13	0.08
All Heated			687	0.073	0.110	0.079	0.083
All Data			1103	0.038	0.101	0.073	0.094

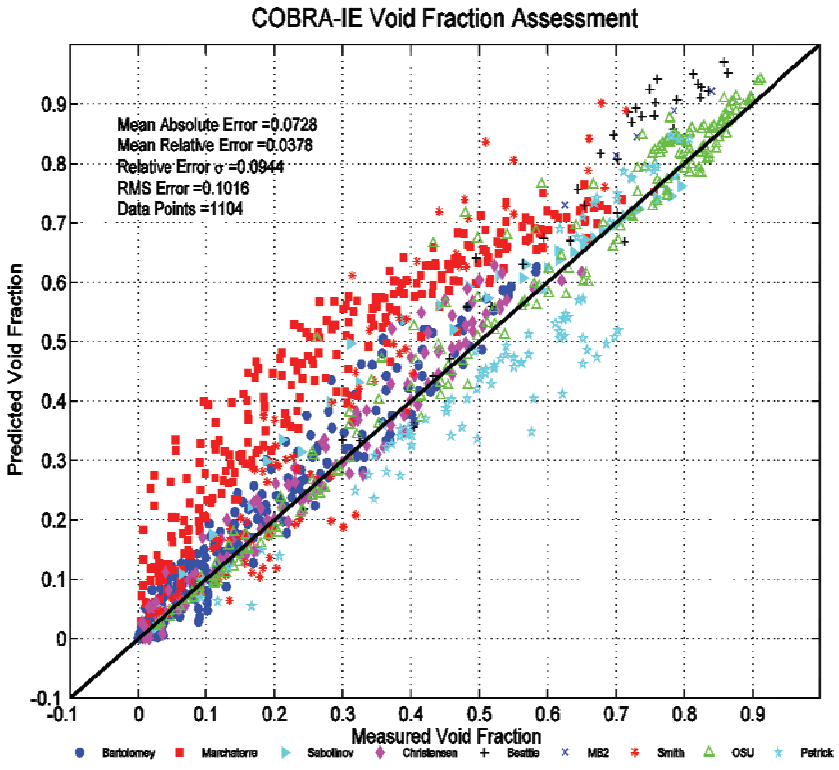

Figure 3 – Comparison of All Data Points

To determine the potential reason for the poor performance of the Marchaterre tests, plots of the error in void fraction prediction were made as a function of pressure and mass flux, Figure 4 and Figure 6. The data shows a clear trend in the boiling cases where the void fraction is overpredicted as the pressure is reduced below 4.3 MPa. To highlight the trend, a boxplot of the void fraction error is presented Figure 5. The vertical dashed lines represent the pressure ranges used for the plot. The figure clearly shows the error increases as pressure is reduced. Additionally, a smaller trend appears to be present in the down-flow, steam-water Petrick data. The fact that the trend is present in the adiabatic cases, indicates that the issue could be with the interfacial shear modeling and is not potentially related to the boiling models used in COBRA-IE.

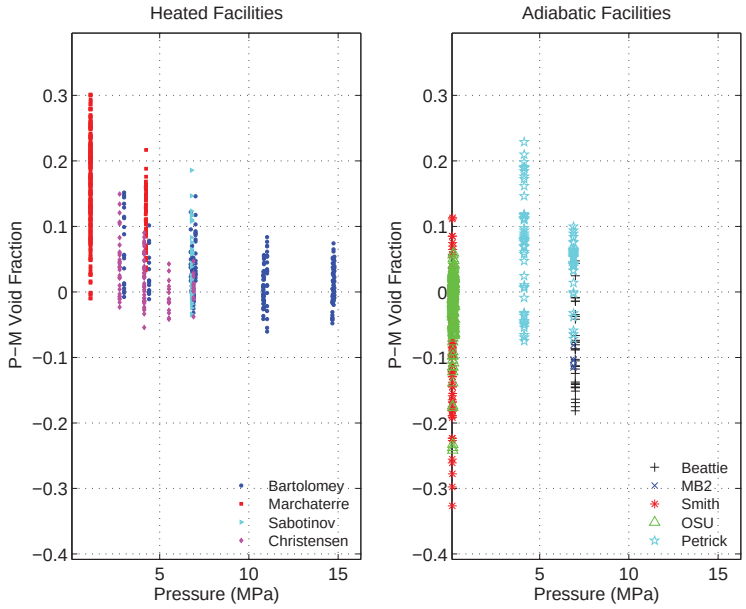

Figure 4 – Error Trends with Pressure

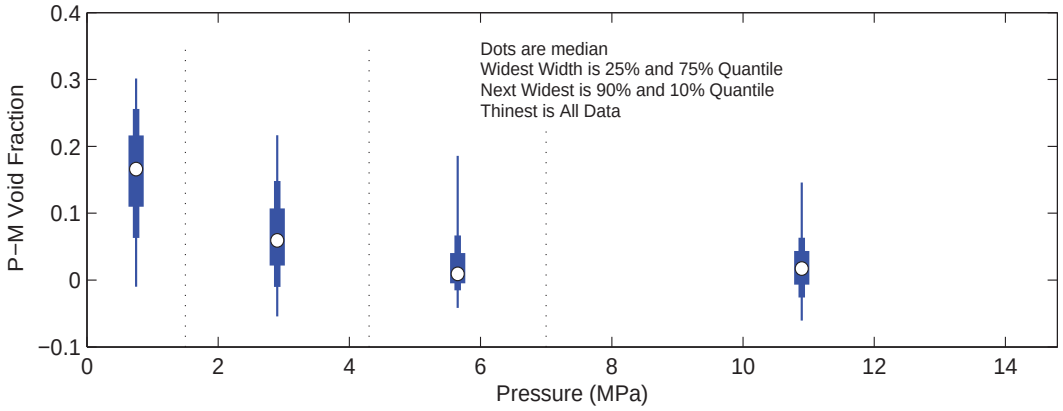

Figure 5 –Boxplot of Error as a Function of Pressure

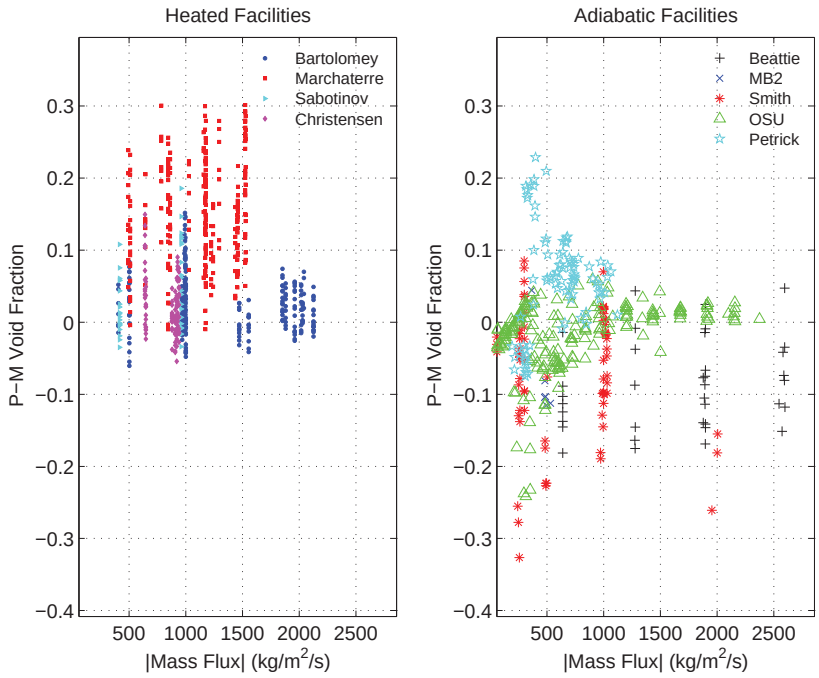

Figure 6 - Error Trends with Mass Flux

No clear correlation of error and mass flux emerges. Instead, the only trend that emerges is that as the mass flux is decreased, the scatter in the error for the Petrick and OSU has a local maximum absolute value of the error at a mass flux of approximately $300\,kg/m^2s$. The COBRA-IE calculated void fraction is larger than the data for the steam-water Petrick data; while the predicted void fractions are smaller for the air-water data. It is not clear what phenomena could simultaneously cause the maximum errors at the same mass flux for these different working fluids while causing the error to have different signs.

The axial void fraction profile predictions for two cases from the Bartolomey test sequence were examined. These two cases were chosen to show a case at high pressure, Figure 7, and a case at lower pressure, Figure 8, where COBRA-IE over predicts the void fraction. For the higher pressure case, the data shows two different slopes in the void fraction as a function of quality data. A lower slope for the subcooled case, and a larger slope for the saturated conditions. The COBRA-IE prediction, which accurately calculates the data at low and high qualities, has a single apparent slope in the same relationship. This creates a maximum error in the predicted values near the location where the equilibrium quality is zero. For the lower pressure case, the COBRA-IE predictions follow the correct trend with equilibrium quality; it is just that the COBRA-IE predictions are translated slightly with respect to quality. Given the very steep slope of the curve at lower pressures, this translation is seen as a large error in the predicted void fraction.

The final trend, presented in Figure 9, is the error for the heated cases as a function of the calculated, mass flow weighted equilibrium quality. This figure shows that the sub-cooled data is well predicted. The interesting trend in these figures is the apparent increase in error as the condition of $X_{eq} = 0$ is approached from either the subcooled or saturated conditions. Note that only data locations where the experimental data indicated the presence of vapor are included in the figure.

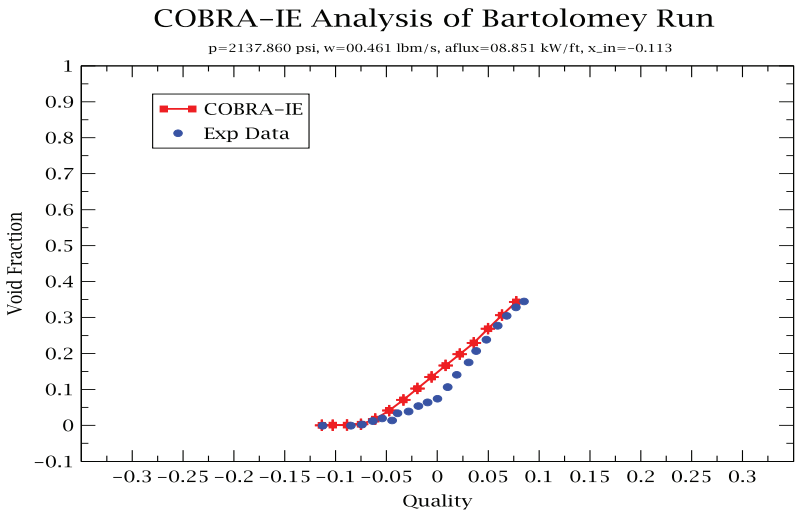

Figure 7 – Bartolomey Case 102 (P = 15 MPa)

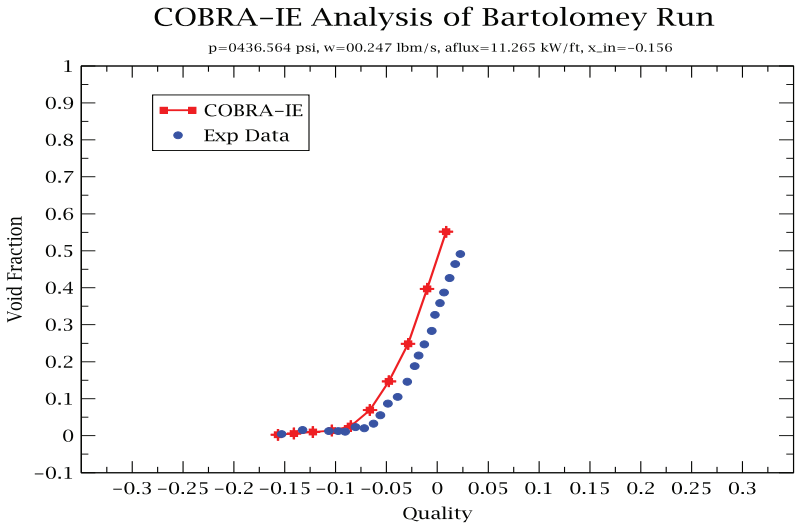

Figure 8 - Bartolomey Case 120 (P = 3 MPa)

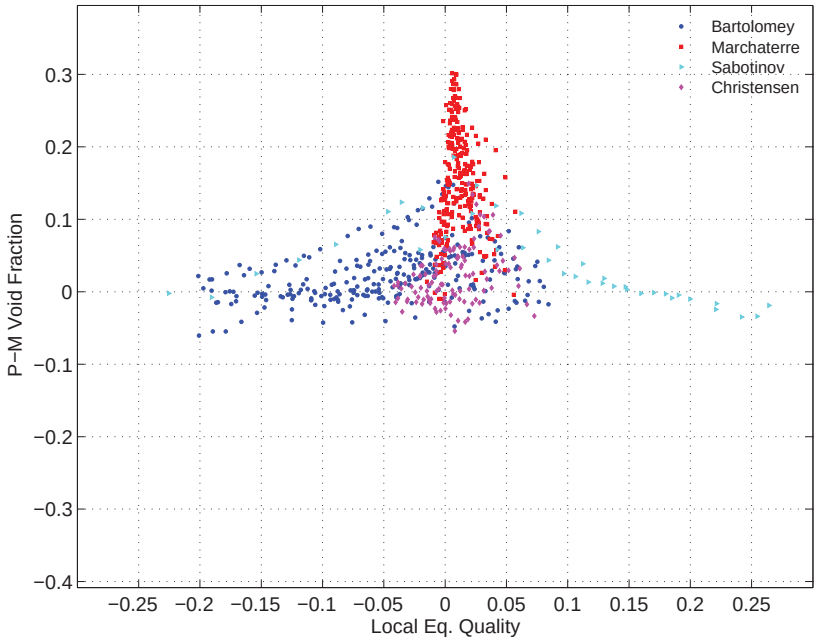

Figure 9 – Error Trends with Local Equilibrium Quality

The clustering of errors near the condition of equilibrium quality of zero implies that interfacial heat and mass transfer terms could be the cause of the misprediction of void fraction. The error structure could be explained if the condensation model were more appropriate for large liquid subcooling values vice small values. If this assumption were true, the condensation would be correctly calculated at large negative equilibrium qualities. The more accurate prediction for the positive qualities would then be the result of a lack of condensation in these conditions.

6. Conclusions

The COBRA-IE analysis code was used to predict void fraction for approximately 1100 data points corresponding to a wide range of conditions. The code was able to predict the data with an average error less than 0.04. The calculations showed a clear trend in that the boiling cases exhibit larger errors as pressure is reduced below 4.3 MPa. Another interesting trend that was seen in the data is that the error in the predictions of void fraction is greatest for equilibrium qualities near zero.

Future work that will be considered as a result of this work could include using the data that was included in this assessment to generate appropriate uncertainty distributions in the pertinent physical models within COBRA-IE for application in a Best-Estimate plus Uncertainty methodology. Additionally, the various deficiencies in the physical models such as interfacial condensation and interfacial drag could be examined to reduce the mean error from the already small value of 0.04.

REFERENCES

1. B.E. Boyack, et al, “Phenomena Identification and Ranking Tables (PIRTs) for Power Oscillations Without Scram in Boiling Water Reactors Containing High Burnup Fuel”, NUREG/CR-6743, (2001)
2. G. B. Wilson, et al, “Phenomena Identification and Ranking Tables for Westinghouse AP600 Small Break Loss-of-Coolant Accident, Main Steam Line Break, Steam Generator Tube Rupture Scenarios”, NUGEG/CR-6541, (1997)

3. B.E. Boyack, et al, “Phenomena Identification and Ranking Tables (PIRTs) for Loss-of-Coolant Accidents in Pressurized and Boiling Water Reactors Containing High Burnup Fuel”, NUREG/CR-6744, (2001)
4. M. Thurgood., et al., “COBRA/TRAC: A Thermal Hydraulic Code for Transient Analysis of Nuclear Reactor Vessels and Primary Coolant Systems,” NUREG/CR 3046 (Volumes 1 5), Pacific Northwest Laboratory (1982)
5. R. Clift and W.H. Gavin, “The Motion of Particles in Turbulent Gas Streams,” *Proc. Chemeca*, **1**, pp 14-28, (1970).
6. J. Kitscha and G. Kocumustafaogullari, “Breakup Criteria for Fluid Particles,” *Int J Multiphase Flow*, **15**, pp 573-588, (1989).
7. J.W. Lane, D.L. Aumiller, F-B Cheung and L.E. Hochreiter, “A Self-Consistent Three-field Constitutive Model Set for Predicting Co-Current Annular Flow”, *Nuclear Eng and Des*, **240**, pp 3294-3308, (2010)
8. J.W. Lane, “The Development of a Comprehensive Annular Flow Modeling Package for Two-Phase Three-Field Transient Safety Analysis Codes” Ph.D Dissertation, Pennsylvania State University, (2009).
9. S.P. Antal et al, “Analysis of Phase Distribution in Fully Developed Laminar Bubbly Two-Phase Flow”, *Int. J. Multiphase Flow*, **17**, pp 635-652, 1991.
10. D Prabhudharwadkar, “Two-Fluid CFD Model of Adiabatic Air-Water Upward Bubbly Flow Through a Vertical Pipe with a One-Group Interfacial Area Transport Equation”, Proceedings of the ASME 2009 Fluids Engineering Division Summer Meeting, August 2-6, Paper FEDSM2009-78306, (2009)
11. I. Kataoka and M. Ishii, "Drift Flux Model for Large Diameter Pipe and New Correlation of Pool Void Fraction", *Int. J. Heat Mass Transfer*, **30**, pp 1927-1939 (1987).
12. Zuber, N and Findlay, J. A., “Average Volumetric Concentration in Two-Phase Flow Systems”, *J. of Heat Transfer*, **87**, pp 453-468 (1965).
13. RELAP Development Team, RELAP5-3D Code Manual, Volume I: Code Structure, System Models and Solution Methods, INEEL-EXT-98-00834, Idaho Falls Idaho, (2007).
14. J. Chen, “A Correlation for Boiling Heat Transfer to Saturated Fluids in Convective Flow,” *ASME 63-HT-34*, (1963).
15. J. Collier and J. Thome, Convective Boiling and Condensation, McGraw-Hill, New York (1996).
16. T. Smith, “Two-Group Interfacial Area Transport Equation in Large Diameter Pipes”, Ph.D. Thesis, Purdue University, (2002).
17. S.M. Bhagwat, “Study Of Flow Patterns and Void Fraction In Vertical Downward Two Phase Flow”, Masters of Science Thesis, Oklahoma Statue University, (2011)
18. D.R.H. Beattie and S. Sugawara, “Steam-Water Void Fraction for Vertical Up-flow in a 73.9 mm Pipe”, *Int. J. Multiphase Flow*, **12**, pp 641-653, (1986).
19. M. Petrick, “A Study of Vapor Carryunder and Associated Problems”, ANL-6581, (1962).
20. K. Takeuchi, M.Y. Young and L.E. Hochreiter, “Generalized Drift Flux Correlation For Vertical Flow”, Nuclear Science and Engineering, **112**, pp 170-180, (1992)
21. H. Christensen, “Power-to-Void Transfer Functions”, ANL-6385, (1961)
22. J.F. Marchaterre, et al, “Natural and Forced-Circulation Boiling Studies”, ANL-5735, (1960)
23. A.S. Devkin and A.S. Podosenov, “RELAP5/MOD3 Subcooled Boiling Model Assessment”, NUREG/IA-0025, (1998)
24. D.L. Aumiller, et al, “Development of Verification Testing Capabilities for Safety Codes”, *Proceedings of NURETH-15*, Paper NURETH15-145, Pisa, Italy (2013).